Smith, D. R., & Calvo, J. M. (1980) *Nucleic Acids Res. 8*, 2255–2274.
Stone, S. R., & Morrison, J. F. (1982) *Biochemistry 21*, 3757–3765.
Stone, S. R., & Morrison, J. F. (1984) *Biochemistry 23*, 2753–2758.
Stryer, L., & Haugland, R. P. (1967) *Proc. Natl. Acad. Sci. U.S.A. 58*, 719–726.
Taira, K., & Benkovic, S. J. (1988) *J. Med. Chem. 31*, 129–137.
Viola, R. E., Cooke, P. F., & Cleland, W. W. (1979) *J. Med. Chem. 96*, 334–340.
Wallace, R. B., Schold, M., Johnson, M. J., Dembeck, P., & Itakura, I. (1981) *Nucleic Acids 9*, 3647.
Wells, J. A., Powers, D. B., Bott, R. R., Graycar, T. P., & Estell, D. A. (1987) *Proc. Natl. Acad. Sci. U.S.A. 84*, 1219–1223.
Winberg, G., & Hammarskjold, M.-L. (1980) *Nucleic Acids Res. 8*, 253–264.
Wu, Y. D., & Houk, K. N. (1987) *J. Am. Chem. Soc. 109*, 2226.
Zoller, M. J., & Smith, M. (1982) *Methods Enzymol. 154*, 329–350.

Functional Consequences of Engineering the Hydrophobic Pocket of Carbonic Anhydrase II†

Carol A. Fierke,* Tiffany L. Calderone, and Joseph F. Krebs
Department of Biochemistry, Duke University Medical Center, Durham, North Carolina 27710
Received May 31, 1991; Revised Manuscript Received August 26, 1991

ABSTRACT: Twelve amino acid substitutions of varying size and hydrophobicity were constructed at Val 143 in human carbonic anhydrase II (including Gly, Ser, Cys, Asn, Asp, Leu, Ile, His, Phe and Tyr) to examine the catalytic roles of the hydrophobic pocket in the active site of this enzyme. The CO_2 hydrase and *p*-nitrophenyl acetate (PNPA) esterase activities, the pK_a of the zinc–water ligand, the inhibition constant for cyanate (K_{OCN}), and the binding constants for sulfonamide inhibitors were measured for various mutants and correlated with the size and hydrophobicity of the substituted amino acid. The k_{cat}/K_M for PNPA hydrolysis and K_{OCN} are linearly dependent on the hydrophobicity of the amino acid at position 143. All of the activities of CAII are decreased by more than a factor of 10^3 when large amino acids (Phe and Tyr) are substituted for Val 143, but the CO_2 hydrase activity is the most sensitive to the size and structure of the substituted amino acid. Addition of a single methyl group (V143I) decreases the activity 8-fold, while substitution of valine by tyrosine essentially destroys the enzyme function (k_{cat}/K_M for CO_2 hydration is decreased by more than 10^5-fold). K_{OCN} does not increase until Phe is substituted for Val 143, suggesting that the cyanate and CO_2 binding sites are not identical. The functional data in conjunction with X-ray crystallographic studies of four of the mutants [Alexander et al., 1991 (following paper in this issue)] allow interpretation of the mutants at a molecular level and mapping of the region of the active site important for CO_2 association. The hydrophobic pocket, including residues Val 121 and Val 143, is important for CO_2 and PNPA association; if the pocket is blocked, substrates cannot approach the zinc–hydroxide with the correct orientation to react. The interaction between Val 143 and CO_2 is relatively weak ($\leq$0.5 kcal/mol) and nonspecific; the association site does not tightly hold CO_2 in one fixed orientation for reaction with the zinc–hydroxide. This mechanism of catalysis may reflect a decreased requirement for specific orientation by CO_2 since it is a symmetrical molecule.

Carbonic anhydrase is a small, monomeric zinc metalloenzyme which catalyzes the reversible hydration of carbon dioxide to bicarbonate and a proton [recent reviews: Coleman (1986), Lindskog (1986), Silverman and Lindskog (1988), and Christianson (1991)]. This enzyme is ubiquitous in living systems, playing a large role in animal and plant metabolism including CO_2 transport, secretory processes, and photosynthesis. Carbonic anhydrase II (CAII)[1] is an extremely efficient catalyst; the second-order rate constant approaches the diffusion-controlled limit ($k_{cat}/K_M^{CO_2} = 1.5 \times 10^8$ M^{-1} s^{-1}) and its turnover number ($k_{cat}^{CO_2} = 1.4 \times 10^6$ s^{-1}) is one of the highest measured. In addition to its CO_2 hydrase activity, CAII will catalyze hydrolysis of many aromatic esters (Pocker & Sarkanen, 1978) and is potently inhibited by aromatic sulfonamides (King & Burgen, 1976).

The three-dimensional structure of human erythrocyte CAII has been solved by X-ray crystallography to 2.0-Å resolution (Liljas et al., 1972) and further refined (Eriksson et al., 1986, 1988a) revealing that the zinc cofactor is located near the center of the enzyme close to the bottom of a 15-Å-deep

†Supported by grants from the National Institutes of Health (GM40602) and the American Cancer Society (JFRA-246) and a Fellowship in Science and Engineering from the David and Lucile Packard Foundation.
*Corresponding author.

[1] Abbreviations: CAII, human carbonic anhydrase II; PNPA, *p*-nitrophenyl acetate; MES, 2-(*N*-morpholino)ethanesulfonic acid; OCN, cyanate; MOPS, 4-morpholinepropanesulfonic acid; TAPS, [tris(hydroxymethyl)methyl]aminopropanesulfonic acid; EDTA, (ethylenedinitrilo)tetraacetic acid; DNSA, dansylamide; ACET, acetazolamide; wt, wild-type; V143G, Val 143 → Gly; V143C, Val 143 → Cys; V143L, Val 143 → Leu; V143I, Val 143 → Ile; V143N, Val 143 → Asn; V143S, Val 143 → Ser; V143H, Val 143 → His; V143F, Val 143 → Phe; V143Y, Val 143 → Tyr; V143D, Val 143 → Asp.

0006-2960/91/0430-11054$02.50/0

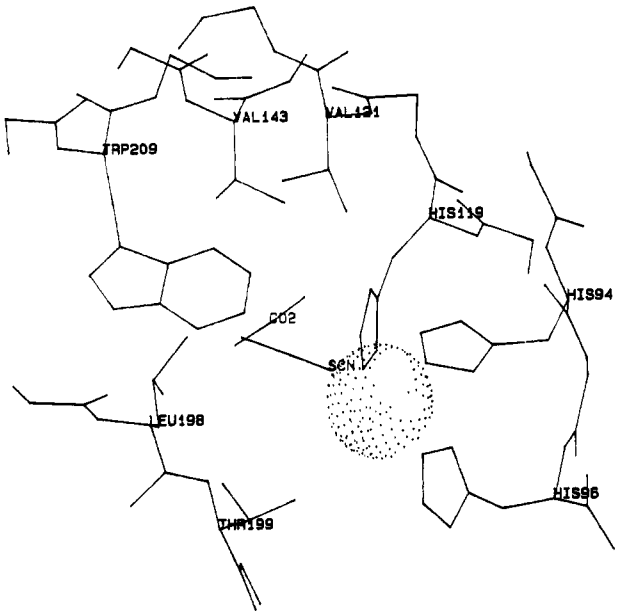

FIGURE 1: Structure of the hydrophobic pocket in the active site of recombinant human carbonic anhydrase II taken from the X-ray crystal structure of Alexander et al. (1991), showing the zinc coordinated to three imidazole ligands, His 94, His 96, and His 119; four amino acids defining the hydrophobic pocket, Val 121, Val 143, Leu 198, and Trp 209; and an essential catalytic residue, Thr 199. The position of thiocyanate (SCN) was determined from a least-squares superposition of the backbone atoms of CAII from the CAII–thiocyanate complex (Eriksson et al., 1988b) with the structure of the recombinant CAII (Alexander et al., 1991) using the software SYBYL (Tripos Associates, Inc.). The position of CO_2 was determined the same way by a superposition of the calculated CAII–CO_2 complex (Merz, 1990, 1991) with the recombinant CAII structure.

active-site cavity. The zinc ion is coordinated to the enzyme by three imidazole groups (His 94, His 96, and His 119) and one solvent molecule in a tetrahedral geometry. The proposed mechanism of catalysis by this enzyme (Silverman & Lindskog, 1988) involves direct nucleophilic attack of the zinc-bound hydroxyl on CO_2 to form a metal-bound bicarbonate and, upon bicarbonate dissociation, an intermediate containing zinc-bound water. This zinc–water species then releases a proton to solvent to regenerate the zinc–hydroxide enzyme. The overall proton transfer occurs in two steps; first, a proton shuttle between zinc–water and His 64 (Steiner et al., 1975; Tu et al., 1989), followed by intermolecular transfer of the proton from His 64 to solvent buffers (Jonsson et al., 1976; Silverman & Tu, 1975).

The active-site cavity is amphiphilic; one wall is dominated by hydrophobic residues and the other by hydrophilic residues. The polar residues, particularly Thr 199 and Glu 106, form a hydrogen-bond network with the zinc-bound hydroxide which functions to stabilize and orient this moiety for nucleophilic attack on CO_2 (Coleman, 1967; Lindskog & Coleman, 1973; Merz, 1990). A set of highly conserved hydrophobic residues (Hewett-Emmett & Tashian, 1991), including Val 121, Val 143, Leu 198, and Trp 209, form a well-defined pocket near the zinc–hydroxide (Figure 1). The catalytic relevance of these nonpolar residues is unclear, although proposed roles include CO_2 binding (Riepe & Wang, 1968; Lindskog, 1986; Liang & Lipscomb, 1990; Merz, 1990, 1991), desolvation of the zinc–hydroxide ligand (Jönsson et al., 1978), and lowering the pK_a of the zinc–water ligand (Woolley, 1977). Although the crystal structure of CAII has been solved (Liljas et al., 1972; Eriksson et al., 1986, 1988a), the CO_2 binding site has not been clearly elucidated. The three-dimensional structure of CAII-bound thiocyanate (Eriksson et al., 1988b) reveals that the inhibitor displaces a water molecule at the mouth of the hydrophobic pocket and interacts with residues Val 143, Leu 198, and Trp 209 (see Figure 1), leading to the proposal that its interactions with the hydrophobic pocket mimic CO_2 binding. This proposed site places CO_2 about 3 Å away from zinc, consistent with the results of a variety of spectroscopic studies which suggest that CO_2 binding to CAII does not involve inner-sphere zinc coordination (Riepe & Wang, 1968; Stein et al., 1977; Williams & Henkens, 1985; Led et al., 1982; Bertini et al., 1979, 1983, 1987). Molecular dynamics and free energy perturbation simulations (Liang & Lipscomb, 1990; Merz, 1990, 1991) also indicate that the hydrophobic pocket may be involved in CO_2 association (see Figure 1). Additionally, the hydrophobic pocket has been implicated in phenyl ester and inhibitor binding from structure–reactivity correlations (Pocker & Beug, 1972; Vedani & Meyer, 1984) and X-ray crystallography (Eriksson et al., 1988b; Vidgren et al., 1990).

Here, we analyze the functional importance of the Val 143 side chain, situated at the base of the hydrophobic pocket, for CO_2 hydration, ester hydrolysis, inhibitor binding and the zinc–water pK_a by determining the properties of a series of mutations at this position. Ten amino acid substitutions at position 143 of CAII were characterized in order to determine the catalytic importance of the size and hydrophobicity of this residue. This analysis shows that a minimal size of the hydrophobic pocket is crucial for the reactivity of both phenyl ester and CO_2 substrates with the active-site zinc–hydroxyl; when the size of the pocket decreases, activity decreases. On the other hand, enlargement of the pocket by removal of the Val 143 side chain has little effect, suggesting that this side chain plays only a minor role in specifically stabilizing the transition state for hydration. The combination of these kinetic results with X-ray crystallographic studies of four of the mutants [Alexander et al., 1991 (following paper in this issue)] allows both detailed mechanistic inferences about the role of the hydrophobic pocket in catalysis and mapping of the region of the pocket involved in substrate association.

Experimental Procedures

Mutagenesis. The cloned CAII gene (Murakami et al., 1987; a generous gift of Dr. W. S. Sly) was placed under T7 regulatory control by inserting it between a T7 late promoter and terminator (Nair et al., 1991; Fierke et al., 1991; Rosenberg et al., 1987). This construct produces recombinant CAII which is identical to blood protein except that the amino terminus is either Met-Ala or Ala [in a similar construct the N-terminal Met has been posttranslationally cleaved in *Escherichia coli* (Forsman et al., 1988)], while it is Ac-Ser in native CAII (Henderson et al., 1976). The recombinant protein appears to be identical to native CAII in activity (Fierke et al., 1991) and structure (Alexander et al., 1991). Oligonucleotide-directed mutagenesis was performed according to the method of Stannsens et al. (1989), except the oligonucleotide concentration was decreased 20-fold, using a 24-base oligonucleotide in which the Val 143 codon (GTT) was replaced by NNC (N is an equal mixture of all four nucleotides). This generates a pool of plasmids containing 15 different amino acids at this position and a new *Sty*I restriction site (NNCCTA GGT). The resulting DNA was transformed into WK6 *mutS* cells. After a second transformation, individual colonies were picked and the DNA was isolated and screened for incorporation of the new *Sty*I site by digestion with restriction endonucleases. The sequence of the codon at amino acid 143 was determined by dideoxy sequencing (Sanger et al., 1977).

Enzyme Induction and Purification. BL21(DE3) cells containing a plasmid encoding mutant CAII were grown and CAII was induced as described (Nair et al., 1991). Cells were pelleted and a crude lysate was prepared by EDTA/lysozyme lysis (Cull & McHenry, 1990) followed by removal of cellular remnants by centrifugation (20000*g*, 45 min). For activity measurements of CAII, this crude extract was then dialyzed extensively against 0.05 M Tris-SO_4, pH 7.4. For protein purification the extract was further fractionated by a 1% streptomycin sulfate precipitation and a 40% ammonium sulfate precipitation. CAII was then precipitated with 90% ammonium sulfate. V143H, V143F, and V143Y mutants were purified to homogeneity by chromatography on an S-Sepharose fast-flow column (2.5 cm × 20 cm) in 0.02 M MES, pH 6.2, eluted with a linear ammonium sulfate gradient (0–0.5 M), followed by a Sephacryl S-100 HR column (2.5 cm × 80 cm) run in 10 mM potassium phosphate buffer, pH 6.5, and 100 mM ammonium sulfate (Y. Xue, B.-H. Jonsson, and S. Lindskog, unpublished data). For V143H and V143Y, a hydroxylapatite column (5 cm × 15 cm) with a linear potassium phosphate (pH 6.5) gradient (5 mM–0.5 M) was necessary to complete the purification. Wild-type, V143G, and V143D CAII proteins were purified using sulfonamide affinity chromatography as previously described (Osborne & Tashian, 1975). The concentration of CAII was determined by measuring the absorbance at 280 nm using a molar absorptivity of 5.4×10^4 M^{-1} cm^{-1} (Coleman, 1967) or by stoichiometric titration with acetazolamide (Williams et al., 1979). The concentration of the E·acetazolamide complex was assayed either by a decrease in the PNPA esterase activity or by a decrease in fluorescence (excitation = 280 nm, emission = 470 nm) in the presence of dansylamide (≤ 2 μM) (Chen & Kernohan, 1967) at concentrations of CAII (≥ 0.5 μM) well above the K_D for acetazolamide. This latter technique was particularly useful for determining the concentration of CAII in crude extracts.

Steady-State Kinetics. The k_{cat}/K_M for CAII-catalyzed PNPA hydrolysis was measured at 25 °C in either 50 mM Tris-SO_4 (pH 7–9) or 50 mM MES (pH 5.5–7), μ = 0.1 with Na_2SO_4, by measuring the change in A_{348}/min ($\Delta\epsilon$ = 5000 M^{-1} cm^{-1}) as a function of PNPA concentration (0–0.5 mM) (Armstrong et al., 1966). Background rates, measured by specifically inhibiting CAII with acetazolamide, were subtracted from the observed rates. To observe the enzyme-catalyzed PNPA hydrolysis for inactive mutants, the enzyme concentration was increased from 0.5 μM (wt) to up to 60 μM (V143F). The pK_a's and pH-independent k_{cat}/K_M's for esterase activity were determined either from a complete pH dependence curve fit to eq 1 using the statistical program SYSTAT (Systat, Inc.) (wt, V143G, V143F, and V143Y) or from the ratio of PNPA hydrolysis at pH 6.5 and 8.0, assuming a single ionizable group (V143D and all enzymes assayed in crude lysates). The esterase activity for V143H did not extrapolate to zero at low pH so eq 2 was used to fit these data.

$$(k_{cat}/K_M)_{obs} = \frac{k_{cat}/K_M}{1 + 10^{(pK_a - pH)}} \quad (1)$$

$$(k_{cat}/K_M)_{obs} = \frac{(k_{cat}/K_M)_1 + (k_{cat}/K_M)_2[10^{(pK_a - pH)}]}{1 + 10^{(pK_a - pH)}} \quad (2)$$

The CO_2 hydration activity of crude lysates was measured at 4 °C by the spectrophotometric assay of Brion et al. (1988), and compared directly to the wild-type activity measured in parallel. The initial rates of CO_2 hydration and HCO_3^- dehydration were measured in a KinTek stopped-flow apparatus (designed by Ken Johnson, Pennsylvania State University) at 25 °C by the changing pH-indicator method (Khalifah, 1971) using the following buffer/indicator pairs: TAPS/*m*-cresol purple (pH 8.5), MES/chlorophenol red (pH 6 and 6.5), and MOPS/*p*-nitrophenol (pH 7.2). The buffer concentration was 50 mM and contained 0.1 mM EDTA, and the enzyme concentration varied from 20 nM (wt) to 90 μM (V143Y) in order to observe catalysis of CO_2 hydration over background. The CO_2 (5–24 mM) and HCO_3^- (10–100 mM) concentrations were varied while the ionic strength was kept constant (μ = 0.1 M) with sodium sulfate. The initial velocity (less than 10% of the reaction) was determined from a least-squares fit of an average of four traces of absorbance versus time. The enzyme-catalyzed rate was determined by subtracting the uncatalyzed rate, measured either in the absence of enzyme or with acetazolamide-inhibited enzyme, from the observed rate. For the solvent isotope effects, the pD in D_2O was calculated from pD = pH + 0.4.

CO_2/HCO_3^- Exchange. The kinetic constants for the CAII-catalyzed exchange between CO_2 and HCO_3^- at equilibrium, k_{cat}^{exch}, $K_{eff}^{HCO_3^-}$, and $k_{cat}^{exch}/K_{eff}^{HCO_3^-}$, were determined using the ^{13}C NMR line-broadening technique (Koenig et al., 1974) as previously described by Simonsson et al. (1979) with the following modifications: buffer conditions used were 0.1 M MES, pH 7.2, μ = 0.2 with Na_2SO_4, 25 °C, in 10% D_2O and the initial enzyme concentration was 140 μM (V143H) or 25 μM (wt). The enzyme was dialyzed against 0.1 M MES, pH 7.2, before the experiment. The background line width was measured both with no CAII and with acetazolamide-inhibited CAII. ^{13}C spectra were obtained on a GN 300 wide-bore spectrophotometer.

Inhibitor Binding Assays. Dansylamide (DNSA) binding constants were determined by measuring an increase in fluorescence (excitation = 280 nm, emission = 470 nm) upon binding of DNSA to CAII (Chen & Kernohan, 1967) at 25 °C in 20 mM potassium phosphate buffer, pH 7.4, using concentrations of CAII less than the observed K_D. Binding constants and error estimates (asymptotic standard error) were determined using the SYSTAT curve-fitting program with eq 3. Acetazolamide (ACET) binding was measured by competition with bound DNSA as a decrease in fluorescence (excitation = 280 nm, emission = 470 nm) indicative of a decrease in the concentration of the E·DNSA complex. The acetazolamide dissociation constant can be calculated from this data using eq 4.

$$Fl = \frac{EP}{1 + \frac{K_{DNSA}}{[DNSA]}} + BF \quad (3)$$

$$Fl = \frac{IF}{1 + \frac{K_{DNSA}}{[DNSA]}\left(1 + \frac{[ACET]}{K_{ACET}}\right)} + BF \quad (4)$$

Fl is the observed fluorescence, EP is the fluorescence endpoint, IF is the initial fluorescence, BF is the background fluorescence, and K_{ACET} and K_{DNSA} are the dissociation constants for acetazolamide and dansylamide, respectively.

The K_{OCN}^{obs} for potassium cyanate was calculated from the inhibition of CAII-catalyzed PNPA hydrolysis at pH 7.53, 50 mM Tris, μ = 0.1 M with Na_2SO_4, using eq 5, where *b* is the background rate of ester hydrolysis:

$$\text{rate} = \frac{k_{cat}/K_M}{1 + [OCN]/K_{OCN}^{obs}} + b \quad (5)$$

Materials. Restriction endonucleases, T4 DNA ligase, and polynucleotide kinase were purchased from New England Biolabs. T4 DNA polymerase was a generous gift from Todd Capson and Stephen Benkovic (Pennsylvania State University). PNPA was obtained from Sigma Chemical Co. Acetazolamide, *p*-nitrophenol, and dansylamide were obtained from Aldrich Chemical Co. Tris base and MES were obtained from Research Organics. $NaH^{13}CO_3$ was purchased from Cambridge Isotopes Lab. Dansylamide and PNPA were purified before use by recrystallization from ethanol and diethyl ether, respectively. All other chemicals were reagent grade.

RESULTS

Mutagenesis and Expression. To investigate the roles of the Val 143 side chain of CAII in catalysis and CO_2 binding, a variety of single amino acid variants at position 143 were constructed and their functional properties characterized. In order to prepare multiple substitutions, oligonucleotide-directed mutagenesis (Stannsens et al., 1989) was performed using an oligonucleotide in which the Val 143 codon (GTT) was replaced with the degenerate codon NNC, which inserts a novel *Sty*I restriction site. This oligonucleotide produces a pool of plasmids encoding 15 amino acids at position 143, excluding only Glu, Gln, Trp, Met, and Lys. The ratio of oligonucleotide to single-strand DNA in the in vitro reactions was decreased to 2:1 in order to maximize the incorporation of varied codons at position 143. After the second transformation, colonies were picked at random and the DNA was purified and digested with *Sty*I to determine if the oligonucleotide was incorporated. Out of 55 colonies tested, 29 contained mutant plasmid, giving a mutagenesis efficiency of 53%. These candidate plasmids were sequenced and 14 unique codons at position 143 were isolated [including two codons for Ser (TCC and AGC) and a second codon for Val (GTC)], encoding 13 amino acid variants (Phe, Leu, Ile, Val, Ser, Pro, Tyr, His, Asn, Asp, Cys, Arg, and Gly). Of these thirteen, two were not pursued further because they formed insoluble inclusion bodies (V143R and V143P). Except for the V143V codon change, which expresses at wild-type levels, expression of the Val 143 variants in *E. coli* was uniformly decreased 3–7-fold. This decrease in expression is not due to use of rare codons since (i) 10 of the 14 codons obtained are classified as optimal codons for *E. coli* (de Boer & Kastelein, 1986) and (ii) the two codons for valine (GTT and GTC) and serine (TCC and AGC) at position 143 produce the same in vivo level of CAII even though they are not both frequently used codons. This result indicates that valine at position 143 is uniquely required for maximal expression of CAII in *E. coli*, and this may be related to protein stability.

Esterase Activity and Zinc–Hydroxyl pK_a. To estimate the importance of Val 143 for phenyl ester binding and hydrolysis and for maintaining the pK_a of the zinc–water ligand, the pH dependence of k_{cat}/K_M for *p*-nitrophenyl acetate (PNPA) hydrolysis was measured for each variant either in crude *E. coli* lysates or in purified protein, as listed in Table I. The observed rate of PNPA hydrolysis is linearly dependent on the concentration of PNPA up to 0.5 mM for all variants, and the activity can be completely inhibited by sulfonamides or anions except for V143H CAII, where one-third of the total observed activity is insensitive to inhibitors. In all cases k_{cat}/K_M was calculated from the difference between the observed enzyme-catalyzed rate and the acetazolamide-inhibited rate. The pH dependence can be described as a simple titration curve for all the purified mutants (except V143H), as illustrated for V143F and V143Y in Figure 2, and this was assumed to be true for all of the other variants. For V143H the acetazolamide-inhibitable esterase activity did not extrapolate to zero at low pH, as shown in Figure 2. The pK_a for this variant was calculated by assuming a decreased specific activity at low pH (eq 2).

Table I: Hydrase and Esterase Activity of CAII Variants at Val 143

mutant	% CO_2 hydrase activity[a]	PNPA hydrolysis	
		k_{cat}/K_M (M^{-1} s^{-1})	pK_a
wt	100	2500 ± 200[a,b]	6.8 ± 0.1[a,b]
V143G[c]	125	1200 ± 100	7.2 ± 0.1
V143C[a]	100	1250 ± 100	6.9 ± 0.1[d]
V143L[a]	51	250 ± 30	6.9 ± 0.1[d]
V143I[a]	36	140 ± 20	6.9 ± 0.1[d]
V143N[a]	34	37 ± 5	6.2 ± 0.2[d]
V143S[a]	17	280 ± 40	7.1 ± 0.2[d]
V143D[c]	7	3 ± 0.3	6.4 ± 0.2[d]
V143H	5	2.7 ± 0.2[b]	6.9 ± 0.2[b]
V143F	0.2	2.1 ± 0.2[b]	7.7 ± 0.2[b]
V143Y	≤0.02	1.8 ± 0.2[b]	7.8 ± 0.1[b]

[a] Specific activity of CAII measured in crude lysates. [b] Activity measured on purified CAII. [c] Taken from Fierke et al. (1991). [d] pK_a estimated from the ratio of activities at two pH's.

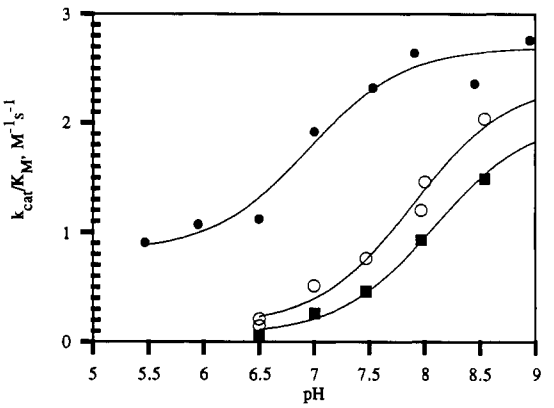

FIGURE 2: pH dependence of the second-order rate constant, k_{cat}/K_M, for the *p*-nitrophenyl acetate esterase activity of three low-activity human carbonic anhydrase II mutants, V143H (●), V143F (○), and V143Y (■), measured at 25 °C in either 50 mM Tris-SO_4 (pH 7–9) or 50 mM MES (pH 5.5–7) with the ionic strength maintained at 0.1 M with sodium sulfate. The solid lines were fit to the data using either eq 1 (V143F and V143Y) or eq 2 (V143H) with the curve-fitting program SYSTAT (Systat, Inc.) using the kinetic parameters listed in Table I as well as $(k_{cat}/K_M)_2$ = 0.8 M^{-1} s^{-1} for V143H.

CO_2 Hydrase Activity. The CO_2 hydrase activity of each substitution was estimated (relative to wild-type) in crude *E. coli* extracts using a qualitative pH-indicator assay in imidazole buffer at an initial CO_2 concentration of about 38 mM (Brion et al., 1988), as shown in Table I. These data suggest that the CO_2 hydration activity is relatively insensitive to changes at position 143; only charged or large amino acid substitutions are extremely detrimental to catalysis. This assay is useful for screening large numbers of CAII mutants but provides limited detailed mechanistic information since both the CO_2 concentration and the pH varies during the assay. Therefore, to further investigate the role of Val 143 in CO_2 hydration, the stopped-flow pH-indicator assay of Khalifah (1971) was used to measure the CO_2 dependence of catalysis in 50 mM TAPS, pH 8.5. Michaelis–Menten kinetics (Segel, 1975) were observed for all the CAII variants, as illustrated for wt (both crude extract and purified protein), V143G, V143H, V143F, and V143Y in Figure 3. The steady-state kinetic parameters for CO_2 hydration were measured for 10 amino acid variants at position 143 as listed in Table II. The kinetic parameters for wild type were identical for purified protein and protein in crude *E. coli* extracts. The solvent isotope effect (k_{H_2O}/k_{D_2O}) on the steady-state kinetic parameters was measured (see

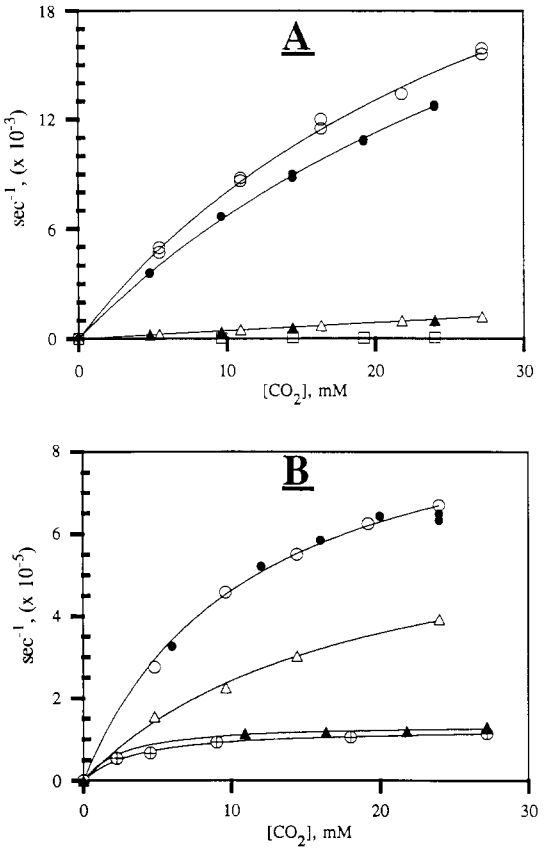

FIGURE 3: Substrate dependence of the CO_2 hydrase activity of human carbonic anhydrase II mutants at position 143. (A) Purified V143H in H_2O (●) and D_2O (○), purified V143F in H_2O (▲) and D_2O (△), and purified V143Y in H_2O (□). (B) Purified wild type in H_2O (●) and D_2O (⊕); wild type in crude extracts in H_2O (○); and purified V143G in H_2O (△) and D_2O (▲). Initial rates for CO_2 hydration were measured using the changing pH-indicator method (Khalifah, 1971) in 50 mM TAPS, pH 8.5, 25 °C. The activity has been corrected for the background rate and the enzyme concentration. The solid lines were fit to the data using the Michaelis–Menten equation (Segel, 1975) with the curve-fitting program SYSTAT using the kinetic parameters listed in Table II and the text.

Table II: Steady-State Kinetic Parameters for CO_2 Hydration of CAII Variants at Val 143[a]

mutant	$k_{cat}/K_M^{CO_2}$ (μM^{-1} s^{-1})	$k_{cat}^{CO_2}$ ($\times 10^{-5}$) (s^{-1})	$K_M^{CO_2}$ (mM)
wt[b,c]	89 ± 7	9.3 ± 0.5	11 ± 1
V143G[b]	38 ± 3	6.9 ± 0.7	18 ± 3
V143C[c]	74 ± 5	10 ± 1	12 ± 1
V143L[c]	15 ± 1	6.2 ± 0.8	42 ± 8
V143I[c]	11 ± 1	10 ± 2	100 ± 24
V143N[c]	13 ± 1	13 ± 5	100 ± 50
V143S[c]	3.9 ± 0.2	≥4[d]	≥100[d]
V143H[b]	0.84 ± 0.014	0.34 ± 0.01	41 ± 2
V143F[b]	0.041 ± 0.006	≥0.08[d]	≥200[d]
V143Y[b]	0.0003 ± 0.0001	≥0.0003[d]	≥100[d]

[a] Activity measured as a function of CO_2 concentration in 50 mM TAPS, pH 8.5, 25 °C, as described in the legend of Figure 3. [b] Activity measured on purified proteins. [c] Activity measured in crude lysates. [d] No curvature in a plot of rate versus $[CO_2]$ up to 24 mM.

Figure 3); the isotope effect on $k_{cat}/K_M^{CO_2}$ was 1.0 ± 0.2 for each variant, while the isotope effect on $k_{cat}^{CO_2}$ was: 4.3 ± 0.3 for wt, 4.6 ± 0.7 for V143G and 0.96 ± 0.13 for V143H. It was not possible to determine the isotope effect on $k_{cat}^{CO_2}$ for V143F since the $K_M^{CO_2}$ is so large. In addition, the kinetic parameters for HCO_3^- dehydration catalyzed by V143H were measured as a function of pH: $k_{cat}/K_M^{HCO_3^-}$ = 0.193 ± 0.006 μM^{-1} s^{-1} (pH 6.0), 0.154 ± 0.011 μM^{-1} s^{-1} (pH 6.5), 0.058 ± 0.006 μM^{-1} s^{-1} (pH 7.2); and $k_{cat}^{HCO_3^-}$ = 7500 ± 200 s^{-1} (pH 6.0), 5700 ± 300 s^{-1} (pH 6.5), 6000 ± 1000 s^{-1} (pH 7.2). The pH dependence of $k_{cat}/K_M^{HCO_3^-}$ can be described as a simple titration curve with a pK_a = 6.8 ± 0.1.

Table III: Inhibitor Binding to CAII Variants at Val 143

mutant	dansylamide[a] K_{DNSA} (μM)	acetazolamide[a] K_{ACET} (nM)	potassium cyanate[b] K_{OCN}^{obs} (μM)
wt[c,d]	1.20 ± 0.05[e]	6.1 ± 0.4[e]	35 ± 1 (5.5)[f]
V143G[c]	1.00 ± 0.03[e]	6.0 ± 0.5[e]	57 ± 8 (18)[f]
V143C[d]	1.26 ± 0.04		81 ± 3 (15)[f]
V143L[d]	9.3 ± 0.2		15 ± 2 (2.8)[f]
V143I[d]	3.2 ± 0.1		17 ± 1 (3.2)[f]
V143N[d]	1.29 ± 0.04		
V143S[d]	2.0 ± 0.1		
V143H[c]	2.5 ± 0.1	12 ± 1	57 ± 3 (11)[f]
V143D[c,e]	5.2 ± 0.2	74 ± 13	
V143F[c]	85 ± 12	1400 ± 200	≥40,000[g] (≥20,000)[f]
V143Y[c]	90 ± 20		

[a] Measured in 0.02 M potassium phosphate buffer, pH 7.4, 25 °C. [b] Measured in 50 mM Tris, pH 7.53, μ = 0.1 with Na_2SO_4, 25 °C. [c] Measured on purified proteins. [d] Measured in crude lysates. [e] Taken from Fierke et al. (1991). Measured under identical conditions. [f] The pH-independent K_{OCN} calculated from $K_{OCN} = K_{OCN}^{obs}/[1 + 10^{(pH-pK_a)}]$. [g] No inhibition of PNPA hydrolysis up to 10 mM cyanate.

The decrease in the isotope effect on $k_{cat}^{CO_2}$ for V143H compared to wild type suggests that the rate-determining step for steady-state turnover may be different for this variant. To verify this result, the kinetic parameters for CAII-catalyzed exchange between CO_2 and HCO_3^- at equilibrium in 0.1 M MES, pH 7.2, 25 °C, using the ^{13}C NMR line-broadening technique (Simonsson et al., 1979), were determined as described under Materials and Methods: $k_{cat}^{exch}/K_{eff}^{HCO_3^-}$ = 4.6 ± 0.7 μM^{-1} s^{-1} (wt), 0.08 ± 0.03 μM^{-1} s^{-1} (V143H); k_{cat}^{exch} = (6.7 ± 1.7) × 10^5 s^{-1} (wt), (0.06 ± 0.02) × 10^5 s^{-1} (V143H); and $K_{eff}^{HCO_3^-}$ = 147 ± 60 mM (wt), 80 ± 20 mM (V143H).

Inhibitor Binding. The dissociation constants for dansylamide binding to CAII (Table III) were measured in 0.02 M phosphate buffer, pH 7.4, as an increase in fluorescence due to fluorescence energy transfer between CAII tryptophans and dansylamide upon binding (Chen & Kernohan, 1967). The dissociation constants for acetazolamide binding (Table III) were measured by competition with dansylamide as a decrease in fluorescence due to the formation of the E·acetazolamide complex. In all cases the data are well fit to a single equilibrium constant as described by eqs 3 and 4. The observed inhibition constants for potassium cyanate (Table III) were measured from inhibition of CAII-catalyzed PNPA hydrolysis in 0.05 M Tris-SO_4, pH 7.53. All the data were well fit to a single, rapid binding equilibrium as described by eq 5, and except for V143H, the background rate at high cyanate concentrations was equal to the rate of PNPA hydrolysis in the absence of CAII. For V143H, one-third of the total activity is not inhibited by cyanate. The values in parentheses in Table III are the estimated pH-independent values for K_{OCN}, describing the binding of cyanate to the zinc–water form of the enzyme, using the pK_a values listed in Table I.

Discussion

The active site of carbonic anhydrase II contains a highly conserved, well-defined hydrophobic pocket composed of Val 121, Val 143, Leu 198, and Trp 209 which has been implicated in substrate (CO_2 and phenyl esters) and inhibitor binding as well as catalysis of CO_2 hydration by desolvation. We have prepared amino acid substitutions at position 143 in human carbonic anhydrase II of varying hydrophobicity and size in order to elucidate the catalytic role of this residue and the functional importance of the hydrophobic pocket. The accompanying paper (Alexander et al., 1991) describes the

three-dimensional structure of four mutants at position 143. The combination of kinetic information with structural data allows a detailed mechanistic understanding of the role of this residue in catalysis.

Esterase Activity and Zinc Water Ionization. The pH dependence of CAII-catalyzed PNPA hydrolysis was measured for 11 amino acid variants at position 143 and the pH-independent k_{cat}/K_M and pK_a were calculated (see Table I). This pK_a is proposed to reflect the ionization of the catalytically important zinc–water ligand since the pH dependence of esterase activity parallels the interconversion between acidic and basic forms of the catalytically active, Co^{2+}-substituted enzyme (Lindskog, 1966). Except for V143H, the pH dependence of the esterase activity of mutants behaves similarly to wild type, suggesting that the observed pK_a is also measuring the equilibrium constant for ionization of the zinc–water ligand. When histidine replaces valine at this position, the sulfonamide-inhibitable activity does not extrapolate to zero at low pH (Figure 2); in fact, about 40% of the activity remains. This behavior could be explained several ways. First, the observed pK_a of 6.9 could reflect the zinc–water ionization (as in wild type) but in this variant the zinc–water form of the enzyme is able to catalyze PNPA hydrolysis using the new histidine as a catalytic residue (perhaps as a general acid catalyst). Alternatively, the pK_a of the zinc–water could be lowered significantly (below 5.5), as is observed for carbonic anhydrase III (Engberg & Lindskog, 1984; Kararli & Silverman, 1985), and the observed pK_a is due to the ionization of the histidine replacement. This latter proposal is unlikely since a single pK_a near 6.8 is observed in HCO_3^- dehydration. Independent measurement of the pK_a of the histidine at 143 or the zinc–water ligand would also distinguish between these two hypotheses.

The hydrophobic pocket has been proposed to be an important component in decreasing the pK_a of the zinc–water ligand in CAII (Woolley, 1977). The data in Table I clearly show that hydrophobicity at position 143 does not cause the observed pK_a to decrease. In fact the opposite trend is observed; two hydrophilic residues (Asp and Asn) lower the pK_a while phenylalanine, a hydrophobic residue, causes an increase in the pK_a. The observed decrease in pK_a for V143D is contrary to the expected result if this were caused solely by an electrostatic interaction; a negative charge positioned near the zinc–hydroxyl moiety should destabilize it relative to zinc–water and cause the pK_a to increase. One possible explanation is that Asp-143 is protonated at neutral pH, having an elevated pK_a in such a hydrophobic environment, and hydrogen-bond donors (such as -COOH or $-CONH_2$) in this position may interact with the active-site hydrogen bond network to stabilize the zinc–hydroxide. Interestingly, the insertion of positive charges at various positions in the hydrophobic region of the active site cause the opposite effect: the observed pK_a increases (J. F. Krebs and C. A. Fierke, unpublished data). Amino acid substitutions at Val 121 at the mouth of the hydrophobic pocket have no effect on the zinc–water ionization (Nair et al., 1991). In addition, the data in Table I clearly show that the rate constant for PNPA hydrolysis is independent of the basicity of the zinc–hydroxyl nucleophile.

On the other hand, the pH-independent k_{cat}/K_M for PNPA hydrolysis (Table I) decreases as the hydrophobicity of the amino acid at residue 143 decreases. This is illustrated in the plot of $\Delta\Delta G^*$ ($\Delta G^*_{mutant} - \Delta G^*_{wt}$) versus hydrophobicity (Figure 4) as measured by the relative distribution coefficient in octanol/water of acetyl amino acids (Fauchère & Pliska, 1983; Eisenberg & McLachlan, 1986). This plot only includes

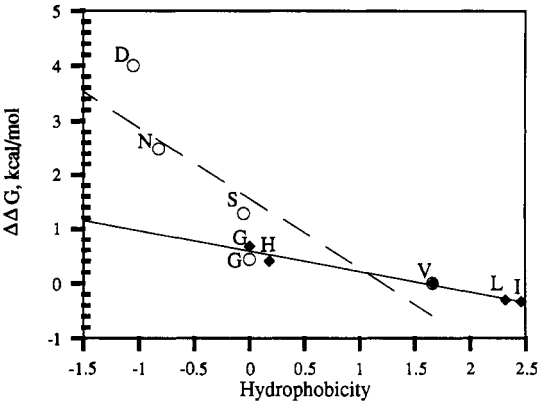

FIGURE 4: Plot of $\Delta\Delta G$ for Val 143 mutants measuring either k_{cat}/K_M for PNPA hydrolysis ($\Delta\Delta G^* = \Delta G^*_{mutant} - \Delta G^*_{wt}$, ○) or K_{OCN}, the cyanate inhibition constant ($\Delta\Delta G = \Delta G_{wt} - \Delta G_{mutant}$, ◆) versus hydrophobicity of the substituted amino acid (1.36π; Eisenberg & McLachlan, 1986). The data are fit to a line using the fitting program SYSTAT (Systat, Inc.): slope = -1.0 ± 0.3 (○) or -0.32 ± 0.05 (◆).

amino acids with side chains smaller than valine since large amino acids appear to have an additional steric effect. The data roughly fit a line with a slope of -1.0 ± 0.3 with V143D falling above the line and V143G falling below the line. This dependence is somewhat larger than either the dependence of PNPA hydrolysis on the hydrophobicity of the amino acid at position 121 (at the mouth of the hydrophobic pocket), as measured by slope = −0.8 (Nair et al., 1991), or the dependence on the hydrophobicity of phenyl ester substrates, slope = −0.5 (Pocker & Beug, 1972).

In addition to the dependence of k_{cat}/K_M for PNPA hydrolysis on hydrophobicity, the rate constant decreases as the size of the amino acid increases. In particular, amino acid substitutions which partially or completely fill the hydrophobic pocket (Alexander et al., 1991) are extremely detrimental to the esterase activity. This effect, along with the hydrophobicity dependence, implicates the hydrophobic pocket as the site for phenyl ester association with the enzyme. In fact, the position of the Tyr 143 side chain [Figure 5; also see Alexander et al. (1991)] with the hydroxyl group near the zinc–solvent ligand may be a good model for the catalytically important association site for PNPA, positioning the acyl group near the nucleophilic zinc–hydroxide. Enlarging the hydrophobic pocket has little effect on catalysis; complete removal of the side chain of valine in V143G CAII causes only a 2-fold decrease in k_{cat}/K_M. Thus, interaction of the valine methyl groups with PNPA provides less than 0.5 kcal/mol stabilization of the transition state for PNPA hydrolysis. This calculation may underestimate the importance of this residue somewhat since compensating structural changes are observed in the V143G variant (Alexander et al., 1991) although the pocket size is still increased considerably (see Figure 5). The valine methyl groups at the mouth of the hydrophobic pocket, Val 121, provide slightly more stabilization of PNPA hydrolysis, 1.4 kcal/mol (Nair et al., 1991).

CO_2 Hydration. The CO_2 hydrase activity of each substitution was estimated (relative to wild type) using a qualitative pH-indicator assay (Brion et al., 1988) as shown in Table I. Surprisingly, in this assay the hydrase activity is quite insensitive to amino acid substitutions. Complete removal of the side chain has no effect and substitution with Cys, Leu, Ile, and Asn causes less than a 3-fold decrease. The only catastrophic substitutions are large amino acids such as Phe and Tyr. These results suggest that specific interactions with the Val 143 side chain play only a minor role in orienting and stabilizing CO_2 during catalysis.

To further elucidate the role of Val 143 in CO_2 hydration by CAII, the steady-state kinetic parameters for CO_2 hydration were measured. Except for the three large substitutions (His, Phe, and Tyr), which decrease both $k_{cat}^{CO_2}$ and $k_{cat}/K_M^{CO_2}$, the mutations at 143 cause a decrease in $k_{cat}/K_M^{CO_2}$ only (up to 20-fold) with little or no decrease in $k_{cat}^{CO_2}$ (less than 2-fold). These data are best interpreted in the framework of the enzymatic mechanism for wild-type CAII (Silverman & Lindskog, 1988). There is considerable evidence that hydration of CO_2 by CAII consists of two steps; CO_2/HCO_3^- interconversion involving the metal center (eq 6) followed by a proton transfer step to re-form the zinc–hydroxyl enzyme which involves first a "proton shuttle" group and then a buffer-dependent reaction (eq 7). The kinetic mechanism in eq 6 incorporates the formation of a CAII–CO_2 complex which may more closely resemble an encounter complex rather than a specific binding site (Jencks, 1975).

$$\text{E-OH}^- \underset{k_{-1}}{\overset{k_1[CO_2]}{\rightleftharpoons}} \text{E-OH}^-\cdot CO_2 \underset{k_{-2}}{\overset{k_2}{\rightleftharpoons}} \text{E-HCO}_3^- \underset{k_{-3}}{\overset{k_3[H_2O]}{\rightleftharpoons}} \text{E-OH}_2 + HCO_3^- \quad (6)$$

$$\text{E-OH}_2 \underset{k_{-4}}{\overset{k_4}{\rightleftharpoons}} {}^+\text{H-E-OH}^- \underset{k_{-5}[BH]}{\overset{k_5[B]}{\rightleftharpoons}} \text{E-OH}^- \quad (7)$$

For this mechanism at pH > 8 and 50 mM buffer, the steady-state kinetic parameter for CO_2 hydration, $k_{cat}^{CO_2}$, equals $k_2k_3k_4/(k_2k_4 + k_{-2}k_4 + k_3k_4 + k_2k_3)$. For wt and V143G, the large solvent isotope effect on $k_{cat}^{CO_2}$ indicates that a proton transfer occurs in the main rate-contributing step. As previously determined for wild type (Silverman & Lindskog, 1988), this step is the intramolecular proton transfer step, k_4. (Therefore, k_2 and k_3 are larger than k_4.) The intramolecular proton transfer (k_4) is also the likely rate-limiting step in $k_{cat}^{CO_2}$ for all the Val 143 substitutions in which $k_{cat}^{CO_2}$ approaches 1×10^6 s^{-1}, including Cys, Ile, Leu, Asn, and Ser. The disappearance of the solvent isotope effect on $k_{cat}^{CO_2}$ for V143H suggests that proton transfer is no longer rate limiting ($k_4 > k_3$ or k_2); hence $k_{cat}^{CO_2} = k_2k_3/(k_2 + k_{-2} + k_3)$. Thus, substitutions at position 143 in the hydrophobic pocket do not affect the rate constant for the intramolecular proton transfer from zinc–water to His 64, which is proposed to occur through a water chain (Venkatasubban & Silverman, 1980). Similarly, little or no effect was observed on $k_{cat}^{CO_2}$ for amino acid substitutions at Val 121 (Nair et al., 1991), leading to the conclusion that the hydrophobic pocket does not play a significant role in ordering the active-site water chain involved in transferring a proton from zinc–water to His 64.

The kinetic parameter $k_{cat}/K_M^{CO_2}$ includes rate constants from CO_2 binding to the first irreversible step, which is HCO_3^- dissociation under initial rate conditions, therefore measuring only the processes in eq 6: $k_{cat}/K_M^{CO_2} = k_1k_2k_3/(k_{-1}k_{-2} + k_{-1}k_3 + k_2k_3) \approx k_1k_2/(k_{-1} + k_2)$ for wild type since $k_{-2} < k_3$ (Lindskog, 1984; Rowlett, 1984). This simplification is likely to be true for the majority of the position 143 mutants since anion binding (Table III), and likely HCO_3^- binding, does not increase significantly. The viscosity dependence of $k_{cat}/K_M^{CO_2}$ for wild type (Pocker & Janič, 1987) suggests that it approaches (within 30%) but does not attain the diffusion-control limit ($k_{-1} \geq k_2$), allowing further simplification of $k_{cat}/K_M^{CO_2} \approx k_1k_2/k_{-1}$. These analyses demonstrate that the effect of a mutation on CO_2 binding and hydration should be readily observed in $k_{cat}/K_M^{CO_2}$.

To further understand the mechanism of CO_2 hydration for the V143H mutant, CO_2/HCO_3^- exchange was measured using the NMR line-broadening technique of Simonsson (1979). The exchange kinetics of this mutant are significantly slower than wild type, indicating that this mutation hinders CO_2/HCO_3^- interconversion. Within experimental error, $k_{cat}^{exch}/K_{eff}^{HCO_3^-}$ is equal to $k_{cat}/K_M^{HCO_3^-}$ for V143H at pH 7.2 as predicted (Simonsson et al., 1979), serving as a control that the NMR exchange technique is yielding relevant kinetic data. The maximal rate constant for exchange, $k_{cat}^{exch} = k_{-1}k_2k_{-2}k_3/(k_{-1}k_2 + k_{-1}k_3 + k_2k_3)(k_2 + k_{-2})$, cannot exceed the rate constant for the slowest step in the exchange. If k_{cat} for either CO_2 hydration or HCO_3^- dehydration is limited by steps in the exchange cycle, this sets an upper limit for k_{cat}^{exch}. When both turnover reactions are limited by steps in the exchange cycle, eq 8 describes the dependence of k_{cat}^{exch} on the turnover parameters (Simonsson et al., 1979). For the V143H mutant this holds true at pH 7.2 since $k_{cat}^{exch} = 6000$ s^{-1}, $k_{cat}^{CO_2} = 23\,000$ s^{-1}, and $k_{cat}^{HCO_3^-} = 6000$ s^{-1}; therefore, the rate-limiting steps for turnover (k_{cat}) involve CO_2 hydration and HCO_3^- dehydration, *not* proton transfer.

$$k_{cat}^{ex} = \frac{k_{cat}^{CO_2}k_{cat}^{HCO_3^-}}{k_{cat}^{CO_2} + k_{cat}^{HCO_3^-}} \quad (8)$$

The steady-state kinetic parameters for V143H can be simplified, given that proton transfer is not rate-limiting for k_{cat} and, since k_{cat}/K_M in both directions is much slower than the diffusion-controlled limit, binding steps are not rate-limiting in k_{cat}/K_M (hence, $k_3 > k_{-2}$ and $k_{-1} > k_2$). If in addition we assume that $k_2 > k_{-2}$, as is true for wild type (Simonsson et al., 1979), then the following simplifications can be made for the pH-independent constants (assuming a pK_a of 6.9): $k_{cat}^{HCO_3^-} \approx k_{cat}^{exch} \approx k_{-2} \approx 7500$ s^{-1} and $K_M^{HCO_3^-} \approx K_{eff}^{HCO_3^-} \approx k_3/k_{-3} \approx 30$ mM. Since the binding constants for bicarbonate (k_3/k_{-3}) and cyanate (Table III) do not increase, we assume that the dissociation rate constant for bicarbonate, k_3, is similar to wild type. If this assumption is valid, then $k_3 > k_2$ and, hence, $k_{cat}^{CO_2} \approx k_2 \approx 3.4 \times 10^4$ s^{-1}; $K_M^{CO_2} \approx k_{-1}/k_1 \approx 40$ mM. For wild type the values of these rate constants can also be estimated: $k_3/k_{-3} \approx 45$ mM, $k_{-2} \approx 3 \times 10^6$ s^{-1}, $k_2 > 3 \times 10^6$ s^{-1}, and $k_{-1}/k_1 \geq 10$ mM (Simonsson et al., 1979; Lindskog, 1984; Rowlett, 1984; Behravan et al., 1990). The conclusion that chemical transformation, CO_2 hydration and bicarbonate dehydration, is the rate-limiting step for turnover in both directions for the V143H mutant is based on several assumptions and is therefore tentative until confirmed by other experimental results. However, these data argue that the histidine substitution at position 143 significantly decreases the catalytic rate constants in both directions without affecting the binding constants. This suggests that substrates can bind to the active site but that the bound complex is less reactive than wild type, due to either decreased reactivity of the zinc–hydroxyl nucleophile or incorrectly bound substrates. For the larger substitutions at this position, V143F and V143Y, $k_{cat}/K_M^{CO_2}$ decreases dramatically, suggesting a decrease either in CO_2 binding (k_1/k_{-1}) or in the reactivity of the bound CO_2 with zinc–hydroxide (k_2).

A comparison of $k_{cat}/K_M^{CO_2}$ for wt and V143G allows an estimation of the stabilization of the transition state for CO_2 hydration relative to unbound CO_2 by the valine methyl groups (≈0.5 kcal/mol). This small amount is similar to the stabilization of CAII-catalyzed PNPA hydrolysis (compared in Figure 6), but these calculations may underestimate the stabilization somewhat due to compensatory contractions of the protein (Alexander et al., 1991). Figure 5 illustrates the interaction between the valine group and CO_2 and shows the hole introduced into the hydrophobic pocket by the glycine. The data also suggest that the exact nature of the side-chain structure is more important for efficient catalysis than hydrophobicity; a plot of $\Delta\Delta G^{\ddagger}$ ($\Delta G^{\ddagger}_{mutant} - \Delta G^{\ddagger}_{wt}$) versus hy-

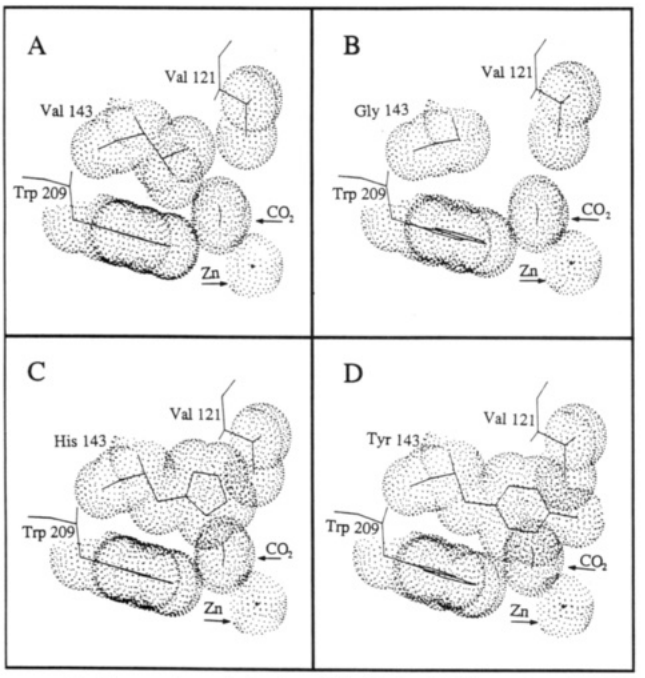

FIGURE 5: Comparison of the size of the hydrophobic pocket of CAII with four different amino acid side chains. Each plot shows Val 121, Trp 209, the amino acid at position 143, the active-site zinc molecule, and the calculated CO_2 binding site determined from a superposition of the calculated CAII–CO_2 complex (Merz, 1990, 1991) with CAII mutant structures (Alexander et al., 1991) as described in Figure 1. The dot structures were calculated by the software SYBYL (Tripos Associates, Inc.) using the van der Waals surface. (A) Structure of wild-type recombinant CAII; (B) structure of mutant CAII with glycine at position 143 (V143G); (C) structure of mutant CAII with histidine at position 143 (V143H); (D) structure of mutant CAII with tyrosine at position 143 (V143Y). In this last plot, the tyrosine side chain clearly overlaps the calculated CO_2 binding site.

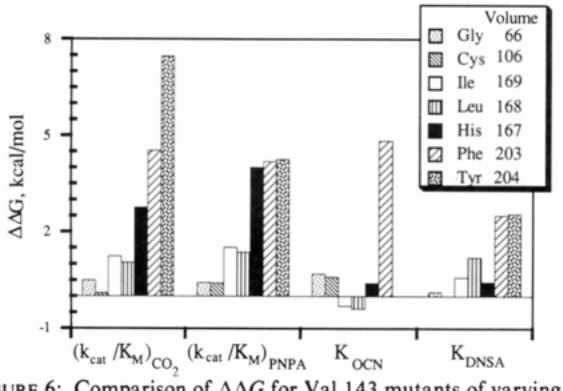

FIGURE 6: Comparison of $\Delta\Delta G$ for Val 143 mutants of varying size (Gly < Cys < Ile ≈ Leu < His < Phe < Tyr) determined either from k_{cat}/K_M for PNPA hydrolysis or CO_2 hydration ($\Delta\Delta G^{\ddagger} = \Delta G^{\ddagger}_{mutant} - \Delta G^{\ddagger}_{wt}$) or from K_{DNSA}, the dissociation constant for dansylamide binding, or K_{OCN}, the cyanate inhibition constant ($\Delta\Delta G = \Delta G_{wt} - \Delta G_{mutant}$). The volumes of the side chains were taken from Richards (1977).

drophobicity for substitution of Val 143 with small side chains (graph not shown) shows *no* observable correlation. The CO_2 hydrase activity of single amino acid mutants at the mouth of the pocket (Val 121) correlates well with the hydrophobicity of a given residue (Nair et al., 1991). This implies that the structural requirements of the active-site surface at the base of the pocket are more constrained.

In particular, the size of the amino acid at position 143 is crucial for catalysis (Figures 6 and 7). Smaller amino acids, like Gly and Cys, form an active-site pocket that functions nearly as well as valine at low CO_2 concentrations, but addition of even a single methyl group (V143I) causes an 8-fold de-

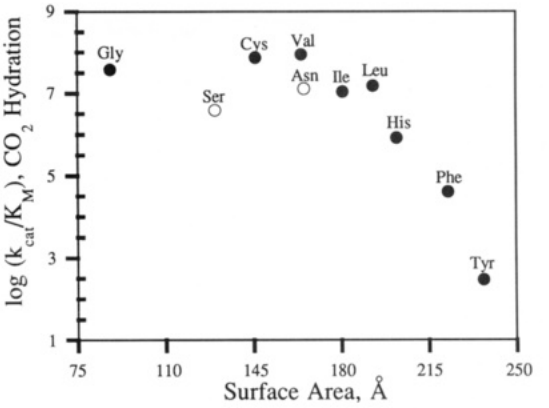

FIGURE 7: Plot of log k_{cat}/K_M for CO_2 hydration for 10 amino acids at position 143 of CAII versus the surface area of the residue (Rose et al., 1985). The open circles indicate hydrophilic amino acids. A similar plot is obtained if the activity is plotted versus the volume (Richards, 1977) of the amino acid side chain.

crease in $k_{cat}/K_M^{CO_2}$ ($\Delta\Delta G^{\ddagger}$ = 1.2 kcal/mol). At high CO_2 concentrations many of the CAII mutants at position 143 have comparable activity since the intramolecular proton transfer step becomes rate limiting. As the size of the amino acid increases further, measured either by surface area (Rose et al., 1985) or by volume (Richards, 1977), the activity decreases precipitously until the V143Y mutant, which is virtually inactive. Figure 6 illustrates that the CO_2 hydrase activity is more sensitive to the size of the side chain than either the esterase activity or inhibitor binding. The three-dimensional structures of the V143H, V143F, and V143Y mutants show the decrease in the depth of the hydrophobic pocket as the size of the amino acid side chain increases (Figure 5; Alexander et al., 1991). The hydroxyl group of tyrosine in V143Y may form a weak hydrogen bond to the zinc–hydroxide, which blocks this group from reacting with substrates in addition to filling the hydrophobic pocket. The position of the tyrosine group is a reasonable site for phenol binding to CAII; phenol is the only known inhibitor that is competitive with CO_2 (Simonsson et al., 1982).

Inhibitor Binding. The hydrophobic pocket has been implicated in inhibitor binding from structure–function correlations (Vedani & Meyer, 1984) and X-ray crystallography (Eriksson et al., 1988b; Vidgren et al., 1990). The sulfonamide group of acetazolamide displaces the zinc–solvent molecule and forms an inner-sphere ligand with zinc and a hydrogen bond with Thr 199. The measured dissociation constants for dansylamide, K_{DNSA}, and acetazolamide, K_{ACET}, suggest that the valine side chains do not interact with either of these inhibitors since complete removal of the side chain to glycine has no effect on binding. This is consistent with the crystal structure of the enzyme–acetazolamide complex (Vidgren et al., 1990). As the side chain increases in size the binding finally decreases, although the majority of the pocket disappears (V143F) before an effect is observed. As shown in Figure 6, sulfonamide binding is less sensitive to the size of the amino acid at position 143 than either CO_2 hydration or PNPA hydrolysis. Although charged amino acids decrease binding, there is no observed correlation between sulfonamide binding and the hydrophobicity of the amino acid at 143.

The crystal structure of CA-bound thiocyanate (Eriksson et al., 1988b) shows that the nitrogen of thiocyanate forms a fifth zinc ligand while the sulfur atom interacts with residues Val 143, Leu 198, and Trp 209 of the hydrophobic pocket (Figure 1). The UV spectra of cyanate bound to cobalt-substituted carbonic anhydrase indicates the zinc remains four-coordinate in this complex. Lindahl et al. (M. Lindahl,

A. Svensson, and A. Liljas, manuscript in preparation) have proposed that cyanate binds in the hydrophobic pocket in the same manner as thiocyanate without entering the inner sphere of zinc coordination, and perhaps mimics CO_2 binding. The inhibition constant for cyanate, K_{OCN}^{obs}, was measured for substitutions at Val 143. Since this inhibitor binds only to the zinc–water form of CAII, the pH-independent inhibition constant, K_{OCN}, was calculated from the pK_a for zinc–water (Table I) for each variant. For wild type, and likely these mutants as well, K_{OCN} is equivalent to the cyanate binding constant (Coleman, 1967). Unlike $k_{cat}/K_M^{CO_2}$, the inhibition constant for cyanate decreases as the hydrophobicity of the residue increases (Figure 4). In addition, a comparison of the effect of substitutions at position 143 on $k_{cat}/K_M^{CO_2}$ and K_{OCN} (Figure 6) clearly shows that the reactivity of CO_2 with zinc–hydroxide is more sensitive to the amino acid size. CO_2 hydration begins to decrease when valine is substituted with either Ile or Leu whereas cyanate binding does not decrease appreciably until the larger Phe is substituted at position 143. This data indicates either that the CO_2 and cyanate binding sites are not coincident and CO_2 interacts with the protein at a site closer to the Val 143 side chain or that CO_2 hydration (k_2) is more sensitive to the active-site milieu than CO_2 and cyanate binding.

Implications for CO_2 Binding and Hydration. Determination of the exact position of, or even the existence of, a CO_2 binding site in CAII has been elusive. A variety of spectroscopic studies, including NMR studies of ^{13}C-labeled substrate binding to CAII (Stein et al., 1977; Williams & Henkens, 1977; Led et al., 1982; Bertini et al., 1979, 1983, 1987) and IR studies (Riepe & Wang, 1968), suggest that CO_2 binding does not involve inner-sphere zinc coordination. In addition, X-ray crystallographic studies of enzyme–inhibitor complexes (Eriksson et al., 1988b) lead to the suggestion that CO_2 binds in the hydrophobic pocket, displacing a fixed water molecule. Theoretical studies of CO_2 binding to CAII (Merz, 1990, 1991; Liang & Lipscomb, 1990) have led to the proposal of a catalytically relevant binding site involving interactions with Val 121, Val 143, Leu 198, and Trp 209. The CO_2 binding site proposed by Merz (1990, 1991) is illustrated in Figure 1 and also overlaid on the hydrophobic pocket of wild type and three mutants, V143G, V143H, and V143Y (Figure 5); the van der Waals surfaces indicate the relative volume of the groups. These pictures suggest that this proposed binding site is consistent with the data; histidine partially overlaps with the proposed site, causing a 100-fold decrease in $k_{cat}/K_M^{CO_2}$, while phenylalanine and tyrosine completely overlap the binding site, causing much larger decreases in activity (10^4–10^5-fold). These decreases in activity due to the blocked hydrophobic pocket can be interpreted as an inability of the CO_2 to approach the zinc–hydroxide with the correct orientation to react due to either complete blockage of the binding site or alteration of the position of the bound CO_2. These results, in conjunction with the crystal structures of the mutant proteins (Alexander et al., 1991), can be used as a molecular ruler to map the region of the active-site cavity necessary for catalytically important CO_2 association.

Although the data are consistent with CO_2 approaching the active-site zinc from the hydrophobic pocket, they also suggest that the interaction of CO_2 with the binding pocket is relatively weak and nonspecific, weaker than the calculated binding energy of −3.4 kcal/mol (Merz, 1991). Removal of valine side chains at either position 121 (Nair et al., 1991) or 143, which increases both the size of the pocket considerably and the amount of solvent in the active site, has little effect on catalysis. Also, CAII with cysteine substituted at position 143 is as active as the wild-type protein. Thus, the data suggest that the hydrophobic pocket is necessary for funneling CO_2 to the zinc–hydroxide; if it is blocked, either partially or completely, the CO_2 cannot approach the zinc with the correct orientation. However, the valine side chains do not interact specifically with the CO_2 molecule to hold it tightly in one fixed orientation, nor is the size of the hydrophobic pocket crucial for desolvation of CO_2 and/or zinc–hydroxide. The symmetry of the linear CO_2 molecule may decrease the requirement for a specific orientation for efficient catalysis.

Implications for Hydrophobic Binding Pockets. Protein engineering of hydrophobic pockets has produced variable results depending on the enzyme. Substitutions in the P1 binding cleft of subtilisin (Estell et al., 1986; Bott et al., 1987) produce large changes in substrate specificity due to a combination of steric hindrance and enhanced hydrophobic interactions. Although the hydrophobic contributions are considerable, these are far outweighed by steric repulsion. In general, the structure of the P1 binding site can be changed dramatically and still produce highly functional proteases. These results mirror the effect of substitutions in the hydrophobic pocket of carbonic anhydrase presented in this work. In contrast, mutations in the hydrophobic pocket of dihydrofolate reductase decrease enzyme activity more specifically (Benkovic et al., 1988; Murphy & Benkovic, 1989). The dissociation constant for dihydrofolate binding to this pocket is dependent on both the hydrophobicity and size of the substituted amino acid, but the rate constant for hydride transfer is optimal only for the wild-type amino acid (Leu); a 50-fold decrease is observed for substitution of four other amino acids (Mayer et al., 1986; Murphy & Benkovic, 1989). These investigations are crucial steps leading to an understanding of protein–substrate interactions in hydrophobic pockets. Comprehension of the plasticity of hydrophobic pockets is essential for protein engineering of novel binding sites and catalytic activities.

Acknowledgments

We thank Drs. William Sly, H.-J. Fritz, and William Studier for their gifts of DNA; Drs. Sven Lindskog, and Bengt-Harold Jonsson for helpful discussions; Drs. Anders Liljas, Kenneth Merz, and David Christianson for coordinates of CAII structures and helpful discussions; Dr. Neil Tweedy and the Duke University Molecular Graphics Facility for help with preparation of the graphics figures; and Ms. Lora LeMosy for help in preparing the manuscript.

References

Alexander, R. S., Nair, S. K., & Christianson, D. W. (1991) *Biochemistry* (following paper in this issue).

Armstrong, J. M., Myers, D. V., Verpoorte, J. A., & Edsall, J. T. (1966) *J. Biol. Chem. 241*, 5137–5149.

Behravan, G., Jonsson, B.-H., & Lindskog, S. (1990) *Eur. J. Biochem. 190*, 351–357.

Benkovic, S. J., Fierke, C. A., & Naylor, A. M. (1988) *Science 239*, 1105–1110.

Bertini, I., Borghi, E., & Luchinat, C. (1979) *J. Am. Chem. Soc. 101*, 7069–7071.

Bertini, I., Canti, G., Luchinat, C., & Borghi, E. (1983) *J. Inorg. Biochem. 18*, 221–229.

Bertini, I., Luchinat, C., Monnanni, R., Roelens, S., & Moratal, J. M. (1987) *J. Am. Chem. Soc. 109*, 7855–7856.

Bott, R., Ultsch, M., Wells, J., Powers, D., Burdick, D., Struble, M., Burnier, J., Estell, D., Miller, J., Graycar, T., Adams, R., & Power, S. (1987) *Biotechnology in Agri-*

cultural Chemistry, ACS Symposium Series 334, pp 139–147, American Chemical Society, Washington, DC.
Brion, L. P., Schwartz, J. H., Zavilowitz, B. J., & Schwartz, G. J. (1988) *Anal. Biochem. 175*, 289–297.
Chen, R. F., & Kernohan, J. C. (1967) *J. Biol. Chem. 242*, 5813–5823.
Christianson, D. W. (1991) *Adv. Protein Chem. 42*, 281–355.
Coleman, J. E. (1967) *J. Biol. Chem. 242*, 5212–5219.
Coleman, J. E. (1986) in *Zinc Enzymes* (Bertini, I., Luchinat, C., Maret, W., & Zeppezauer, M., Eds.) pp 49–58, Birkhauser, Boston.
Cull, M., & McHenry, C. S. (1990) *Methods Enzymol. 182*, 147–153.
de Boer, H. A., & Kastelein, R. A. (1986) in *Maximizing Gene Expression* (Reznikoff, W., & Gold, L., Eds.) pp 225–285, Butterworths, Boston.
Eisenberg, D., & McLachlan, A. D. (1986) *Nature 319*, 199–203.
Engberg, P., & Lindskog, S. (1984) *FEBS Lett. 170*, 326–330.
Eriksson, A. E., Jones, T. A., & Liljas, A. (1986) in *Zinc Enzymes* (Bertini, I., Luchinat, C., Maret, W., & Zeppezauer, M., Eds.) pp 317–328, Birkhauser, Boston.
Eriksson, A. E., Jones, T. A., & Liljas, A. (1988a) *Proteins: Struct., Funct., Genet. 4*, 274–282.
Eriksson, A. E., Kylsten, P. M., Jones, T. A., & Liljas, A. (1988b) *Proteins: Struct., Funct., Genet. 4*, 283–293.
Estell, D. A., Graycar, T. P., Miller, J. V., Powers, D. B., Burnier, J. P., Ng, P. G., & Wells, J. A. (1986) *Science 233*, 659–663.
Fauchère, J.-L., & Pliska, V. (1983) *Eur. J. Med. Chem. 18*, 369–375.
Fierke, C. A., Krebs, J. F., & Venters, R. A. (1991) in *International Workshop on Carbonic Anhydrase: From Biochemistry and Genetics to Physiology and Clinical Medicine* (Botrê, F., Gros, G., & Storey, B. T., Eds.) pp 22–36, VCH, Weinheim, Germany.
Forsman, C., Behravan, G., Jonsson, B.-H., Liang, Z.-W., Lindskog, S., Ren, X., Sandström, J., & Wallgren, K. (1988) *FEBS Lett. 229*, 360–362.
Henderson, L. E., Henriksson, D., & Nyman, P. O. (1976) *J. Biol. Chem. 251*, 5457–5463.
Hewett-Emmett, D., & Tashian, R. E. (1991) in *The carbonic anhydrases: Cellular physiology and molecular genetics* (Dodgson, S. J., Gros, G., Carter, N. D., & Tashian, R. E., Eds.) Plenum, New York (in press).
Jencks, W. P. (1975) *Adv. Enzymol. Relat. Areas Mol. Biol. 43*, 219–410.
Jonsson, B.-H., Steiner, H., & Lindskog, S. (1976) *FEBS Lett. 64*, 310–314.
Jönsson, B., Karlström, G., & Wennerström, H. (1978) *J. Am. Chem. Soc. 100*, 1658–1661.
Kararli, T., & Silverman, D. N. (1985) *J. Biol. Chem. 260*, 3484–3489.
Khalifah, R. G. (1971) *J. Biol. Chem. 246*, 2561–2573.
King, R. W., & Burgen, A. S. V. (1976) *Proc. R. Soc. B 193*, 107–125.
Koenig, S. H., Brown, R. D., London, R. E., Needham, T. E., & Matwiyoff, N. A. (1974) *Pure Appl. Chem. 40*, 103–113.
Led, J. J., Neesgaard, E., & Johansen, J. T. (1982) *FEBS Lett. 147*, 74–80.
Liang, J.-Y., & Lipscomb, W. N. (1990) *Proc. Natl. Acad. Sci. U.S.A. 87*, 3675–3679.
Liljas, A., Kannan, K. K., Bergstên, P.-C., Waara, I., Fridborg, K., Strandberg, B., Carlbom, U., Järup, L., Lövgren, S., & Petef, M. (1972) *Nature New Biol. 235*, 131–137.
Lindskog, S. (1966) *Biochemistry 5*, 2641–2646.
Lindskog, S. (1984) *J. Mol. Catal. 23*, 357–368.
Lindskog, S. (1986) in *Zinc Enzymes* (Bertini, I., Luchinat, C., Maret, W., & Zeppezauer, M., Eds.) pp 307–316, Birkhauser, Boston.
Lindskog, S., & Coleman, J. E. (1973) *Proc. Natl. Acad. Sci. U.S.A. 70*, 2505–2508.
Mayer, R. J., Chen, J.-T., Taira, K., Fierke, C. A., & Benkovic, S. J. (1986) *Proc. Natl. Acad. Sci. U.S.A. 83*, 7718–7720.
Merz, K. M., Jr. (1990) *J. Mol. Biol. 214*, 799–802.
Merz, K. M., Jr. (1991) *J. Am. Chem. Soc. 113*, 406–411.
Murakami, H., Marelich, G. P., Grubb, J. H., Kyle, J. W., & Sly, W. S. (1987) *Genomics 1*, 159–166.
Murphy, D. J., & Benkovic, S. J. (1989) *Biochemistry 28*, 3025–3031.
Nair, S. K., Calderone, T. L., Christianson, D. W., & Fierke, C. A. (1991) *J. Biol. Chem. 266*, 17320–17325.
Osborne, W. R. A., & Tashian, R. E. (1975) *Anal. Biochem. 64*, 297–303.
Pocker, Y., & Beug, M. W. (1972) *Biochemistry 11*, 698–707.
Pocker, Y., & Sarkanen, S. (1978) *Adv. Enzymol. Relat. Areas Mol. Biol. 47*, 149–274.
Pocker, Y., & Janjič, N. (1987) *Biochemistry 26*, 2597–2606.
Richards, F. M. (1977) *Annu. Rev. Biophys. Bioeng. 6*, 151–176.
Riepe, M. E., & Wang, J. H. (1968) *J. Biol. Chem. 243*, 2779–2787.
Rose, G. D., Geselowitz, A. R., Lesser, G. J., Lee, R. H., & Zehfus, M. H. (1985) *Science 229*, 834–838.
Rosenberg, A. H., Lade, B. N., Chui, D.-S., Lin, S.-W., Dunn, J. J., & Studier, F. W. (1987) *Gene 56*, 125–135.
Rowlett, R. S. (1984) *J. Protein Chem. 3*, 369–393.
Sanger, F., Nicklen, S., & Coulson, A. R. (1977) *Proc. Natl. Acad. Sci. U.S.A. 74*, 5463–5467.
Segel, I. H. (1975) *Enzyme Kinetics*, John Wiley and Sons, New York.
Silverman, D. N., & Tu, C.-K. (1975) *J. Am. Chem. Soc. 97*, 2263–2269.
Silverman, D. N., & Lindskog, S. (1988) *Acc. Chem. Res. 21*, 30–36.
Simonsson, I., Jonsson, B.-H., & Lindskog, S. (1979) *Eur. J. Biochem. 93*, 409–417.
Simonsson, I., Jonsson, B.-H., & Lindskog, S. (1982) *Biochem. Biophys. Res. Commun. 108*, 1406–1412.
Stanssens, P., Opsomer, C., McKeown, Y. M., Kramer, W., Zabeau, M., & Fritz, H.-J. (1989) *Nucleic Acids Res. 17*, 4441–4454.
Stein, P. J., Merrill, S. P., & Henkens, R. W. (1977) *J. Am. Chem. Soc. 99*, 3194–3196.
Steiner, H., Jonsson, B.-H., & Lindskog, S. (1975) *Eur. J. Biochem. 59*, 253–259.
Tu, C.-K., Silverman, D. N., Forsman, C., Jonsson, B.-H., & Lindskog, S. (1989) *Biochemistry 28*, 7913–7918.
Vedani, A., & Meyer, E. F., Jr. (1984) *J. Pharm. Sci. 73*, 352–358.
Venkatasubban, K. S., & Silverman, D. N. (1980) *Biochemistry 19*, 4984–4989.
Vidgren, J., Liljas, A., & Walker, N. P. C. (1990) *Int. J. Biol. Macromol. 12*, 342–344.
Williams, T. J., & Henkens, R. W. (1985) *Biochemistry 24*, 2459–2462.
Williams, J. W., Morrison, J. F., & Duggleby, R. G. (1979) *Biochemistry 18*, 2567–2573.
Woolley, P. (1977) *J. Chem. Soc., Perkins Trans. 2*, 318–324.